

**Synergistic Cytotoxic Effect of *Annona muricata* and *Caesalpinia sappan* Nanoparticles via Expression of BAD Pro-Apoptotic Protein in HeLa Cervical Cancer Cells**Okid P. Astirin<sup>1</sup>, Adi Prayitno<sup>2</sup>, Anif N. Artanti<sup>3</sup>, Elisa Herawati<sup>1\*</sup>, Anggraini R. Dewi<sup>1</sup>, Virnanda R. Aryani<sup>1</sup>, Vector S. Dewangga<sup>1</sup><sup>1</sup>Department of Biology, Faculty of Mathematics and Natural Sciences, Sebelas Maret University, Surakarta, Indonesia<sup>2</sup>Department of Pathobiology, Faculty of Medicine, Sebelas Maret University, Surakarta, Indonesia<sup>3</sup>Department of Pharmacy, Vocational College, Sebelas Maret University, Surakarta, Indonesia

## ARTICLE INFO

## ABSTRACT

## Article history:

Received 20 October 2021

Revised 14 November 2021

Accepted 04 December 2021

Published online 03 January 2022

**Copyright:** © 2021 Astirin *et al.* This is an open-access article distributed under the terms of the [Creative Commons Attribution License](https://creativecommons.org/licenses/by/4.0/), which permits unrestricted use, distribution, and reproduction in any medium, provided the original author and source are credited.

*Annona muricata* and *Caesalpinia sappan* are among the most important traditional medicinal plants, which contain numerous chemicals with various pharmacological properties. Although extracts from both plants have demonstrated anticancer activity, there has been no report on the anticancer effect of the combination of *A. muricata* and *C. sappan* nanoparticles particularly on cervical cancer (HeLa) cells. This study aimed to determine the optimum combination dose of both nanoparticles that showed a synergistic effect to induce apoptosis in HeLa cells. The nanoparticles were prepared using *A. muricata* leaves and *C. sappan* heartwood using the glass ionic method. Immunostaining was performed to evaluate the expression of pro-apoptotic marker BAD (BCL2 associated agonist of cell death) protein. Cytotoxicity effect was tested using the 3-(4,5-dimethylthiazol-2-yl)-2,5-diphenyl-2H-tetrazolium bromide (MTT) assay. The size of the nanoparticles ranged between 237-453 nm and showed polydispersity index of 0.354 (*A. muricata*) and 0.486 (*C. sappan*), which means that the level of nanoparticle size distribution is quite uniform. BAD acts as an essential mediator of intrinsic apoptosis, as shown by enhanced expression of BAD in the group of cells treated with the nanoparticles. The employment of two nanoparticles dose combinations showed a synergistic cytotoxic effect (Combination Index < 1) when each nanoparticle concentration was given at ½ IC<sub>50</sub> (*C. sappan*) and ¼ IC<sub>50</sub> (*A. muricata*), resulting in 52.51% of cell viability. The synergistic effect exhibited by *A. muricata* and *C. sappan* nanoparticles suggests a possible different target or signaling pathway that results in a reduction of required nanoparticles concentrations for individual sample.

**Keywords:** *Annona muricata*, *Caesalpinia sappan*, Nanoparticle, BAD protein, Cytotoxicity.

**Introduction**

Cervical cancer is a primary cancer caused by infection of the high-risk (oncogenic) type of Human Papillomavirus (HPV) into the cells that coat the cervix surface. HPV types 16 and 18 with oncogenes E6 and E7 induce severe dysplasia, which can develop into cervical intraepithelial neoplasia.<sup>1</sup> The clinical uses of anticancer drugs is usually accompanied by several unwanted effects,<sup>2,3</sup> therefore, the search for new anticancer agents with better efficacy, selective toxicity, and fewer side effects against cervical cancer cells is a continuous effort. Plant-derived phytochemicals have served us well in combating many types of cancer. Studies conducted in vitro using extracts from two medicinal plants, *Annona muricata* and *Caesalpinia sappan*, show that both were potential anticancer agents.<sup>4-6</sup> Crude aqueous extract and chloroform-ethyl acetate fraction of *Annona muricata* L. leaves inhibited proliferation of MCF-7 (breast) and HeLa (cervix) cancer cells, suggesting the presence of anticancer compounds in these extracts.<sup>7,8</sup>

\*Corresponding author. E mail: [elisahera@staff.uns.ac.id](mailto:elisahera@staff.uns.ac.id)  
Tel: +62-271-663375

**Citation:** Astirin OP, Prayitno A, Artanti AN, Herawati E, Dewi AR, Aryani VR, Dewangga VS. Synergistic Cytotoxic Effect of *Annona muricata* and *Caesalpinia sappan* Nanoparticles via Expression of BAD Pro-Apoptotic Protein in HeLa Cervical Cancer Cells. Trop J Nat Prod Res. 2021; 5(12):2108-2114. [doi.org/10.26538/tjnpr/v5i12.11](https://doi.org/10.26538/tjnpr/v5i12.11)

Official Journal of Natural Product Research Group, Faculty of Pharmacy, University of Benin, Benin City, Nigeria.

The compounds are produced from secondary metabolic processes consisting of alkaloids, flavonoids, triterpenoids/steroids, and acetogenins belonging to the polyketide group. However, acetogenins are the major class of compounds studied from the perspective of anticancer activity. Acetogenins halted the cell at the G2/M phase, induced mitochondrial damage and apoptosis, and promoted nuclear translocation of apoptosis-inducing factors.<sup>9,10</sup>

*Caesalpinia sappan* L. heartwood also induces endometrial cell death by regulating phosphorylation of pyruvate dehydrogenase.<sup>11</sup> In HeLa cells, methanol extract of *C. sappan* at IC<sub>50</sub> value of 26.5±3.2 g/mL induces apoptosis as indicated by DNA fragmentation and activation of the caspase-3 enzyme.<sup>12</sup> *C. sappan* heartwood also induces apoptosis in other types of cancer cells, e.g., T24 human bladder cancer cells<sup>13</sup> and K562 leukemia cells.<sup>14</sup> The major biologically active compound from *C. sappan* heartwood is brazilin, which readily transformed into brazilein upon oxidation.<sup>15</sup> Tao *et al.*<sup>16</sup> showed that brazilin isolated from *C. sappan* increased the sensitivity of doxorubicin-resistant leukemia cells K562 and K562/AO2 during chemotherapy.

The family of Bcl-2 proteins, i.e., BAD (Bcl-2 Associated Death Promoter), is one of the primary regulators of the mitochondria-mediated pathway to apoptosis.<sup>17,18</sup> Impaired apoptosis eventually leads to expansion of cancerous cells and altered expression of molecular determinants of apoptosis, such as BAD that has a detrimental outcome. Yu *et al.*<sup>19</sup> reported that downregulation of BAD shows a worse outcome in patients with small lung carcinoma, thus, BAD can serve as a marker and target molecule for cancer therapy. In the event of apoptosis, BAD will suppress the expression of Bcl-2, changing the mitochondrial membrane integrity and triggering the activation of the caspase cascade. The active caspase cascade will trigger the activity in DNA-se, which then enters the

nucleus and damages cell DNA, resulting in programmed cell death known as the mechanism of apoptosis.<sup>20,21</sup> The design of nanotechnology-based anticancer agents can target specific and promote intracellular uptake of HeLa cells.<sup>22</sup> Chitosan, a natural biopolymer, is often used to formulate nanoparticles because it has good biocompatibility that can increase membrane permeability.<sup>23,24</sup> Fractions of *A. muricata* and *C. sappan* formulated with nanotechnology can monitor disease progression using carbon nanotubes, nanotechnology-based sensors, and also serve as drug delivery systems.<sup>25</sup> Nevertheless, reports on the development of nanoparticles from these medicinal plants are still limited. In the present study, nanoparticles from the active fractions of *A. muricata* and *C. sappan* were developed, and both were subjected to cytotoxicity assay in HeLa cells to examine their synergistic effect. BAD acts as an essential mediator of intrinsic apoptosis. Dose combination of both nanoparticles accelerated apoptosis in the HeLa cells, suggesting a possible different target or signaling pathway that results in a reduction of required nanoparticles concentrations for each sample.

## Materials and Methods

### Plant materials, collection, and identification

The plant specimens were obtained from the Research and Development Center for Medicinal Plants and Traditional Medicines of the Health Research and Development Agency in Central Java, Indonesia between July to September 2018. The plant's specimens were authenticated by Mr. Suratman Suratman (a taxonomist), Department of Biology, Sebelas Maret University. A voucher specimen of these plants has been deposited in the Herbarium Soloense, Department of Biology, Sebelas Maret University with Reference no: 077 /UN27.9.6.4/Lab/2021 for future reference.

### Fractionation of *A. muricata* and *C. sappan* L.

Previous study<sup>4</sup> showed that chloroform was the most effective solvent to isolate the fraction of *A. muricata* with the highest cytotoxicity. Thus, in this study, *A. muricata* leaves were fractionated using chloroform. The *C. sappan* heartwood samples were extracted using ethanol according to a method by Kim.<sup>11</sup> Next, the column chromatography method was used to fractionate the *C. sappan* heartwood extract based on the method described elsewhere.<sup>26</sup>

### Thin-layer chromatography

Thin-layer chromatography (TLC) analysis was performed using TLC plate (F254 Silica gel 60). The mobile phase of *A. muricata* fraction was n-hexane: ethyl acetate = 8:2 v/v and *C. sappan* fraction was chloroform: methanol = 5:1 v/v. The Retention Factor (RF) values were calculated from separated compounds on the TLC plate. Chamber with iodine crystals was prepared to keep the TLC plates for a few seconds. Iodine reacted with the mobile phase and metabolites, making it visible under the UV light after a few seconds.<sup>26</sup>

### Synthesis of nanoparticles

An ultrasonicator was used to formulate nanoparticles of *A. muricata* and *C. sappan* using the glass ionic method between chitosan and NaTPP (sodium tripolyphosphate).<sup>27</sup> A preliminary study conducted by our group showed the optimum nanoparticle formula of 12.5 mg *A. muricata* leaf fraction dissolved in 125  $\mu$ L of Dimethyl Sulfoxide (DMSO) and 12.5 mg *C. sappan* heartwood fraction dissolved in 200  $\mu$ L of distilled water. Each fraction solution was added with 0.2% chitosan and homogenized by a vortex. These mixtures were then mixed with 0.1% NaTPP solution drip while stirred at 400 rpm (25°C) until all the NaTPP solution dissolved.<sup>27</sup> The Design-Expert software<sup>28</sup> was used to optimize the nanoparticle composition.

### Determination of particle size, measurement of transmittance, and zeta potential

The nanoparticle size of *A. muricata* leaf and *C. sappan* heartwood, also zeta potential were determined by dispersing the particles with distilled water (1:1 v/v) at 25°C and measured using Nanopartica SZ-

100 (Horiba). The PSA (dynamic light scattering method) was used to test the particle size and zeta potential. The particle size distribution was inspected with DLS analyzer with an outcome of Polydispersion Index (PI). PI value lesser than one represents a good polydispersion. A UV-Vis spectrophotometer with a wavelength of 650 nm was used to measure the nanoparticle's transmittance.<sup>27</sup>

### Cell culture and cytotoxicity assay

HeLa cells used in this study were obtained from the Integrated Research and Testing Laboratory, Gadjah Mada University. The cells were routinely cultured using RPMI 1640 (Gibco) medium supplemented with 10% FBS in an incubator with 5% CO<sub>2</sub> and 37°C. The MTT assay or colourimetric cell viability with 3-[4,5-dimethylthiazol-2-yl] - 2,5 diphenyl tetrazolium bromide was used to test the cell's cytotoxicity.<sup>4</sup> In this method, nanoparticles were diluted using RPMI medium at various concentrations; 285.5, 142.75, 71.37, 57.1  $\mu$ g/mL for *A. muricata* and 44, 22, 11, 8.8  $\mu$ g/mL for *C. sappan* heartwood. The MTT reagent (0.5 mg/mL Phosphate Buffered Saline) was diluted in RPMI culture medium. The medium was supplemented with 1% (w/w) penicillin-streptomycin (Gibco, Invitrogen USA) and 10% Fetal Bovine Serum (FBS Qualified, Gibco, Invitrogen USA). HeLa cells were incubated at 37°C and 5% CO<sub>2</sub>. Colourimetric assay ELISA was used to measure absorbancy with a wavelength of 595 nm. Each experiment was performed in triplicates.

### Combination Indices

The combination index (CI) between the nanoparticles from *A. muricata* and *C. sappan* heartwood was calculated using the equation:

“ same mode of action “

$$IK = \frac{(D)1}{(Dx)1} + \frac{(D)2}{(Dx)2}$$

“different mode of action “

$$IK = \frac{(D)1}{(Dx)1} + \frac{(D)2}{(Dx)2} + \frac{(D)1(D)2}{(Dx)1(Dx)2}$$

where:

(D)1: concentration of soursop leaf fraction combination treatment

(Dx)1: single treatment concentration of soursop fraction with D1 response

(D)2: concentration of sappan wood fraction combination treatment

(Dx)2: single treatment concentration of the sappan wood fraction with the D2 response

Microsoft Excel was used to calculate the CI values using linear regression of the combined log test concentration.<sup>29</sup> The interpretation of CI value was based on Reynolds & Maurer<sup>30</sup> (see Supplementary Table S1).

### Immunostaining

The immunostaining procedure was slightly modified from earlier study.<sup>31</sup> Briefly, HeLa cells grown on the coverslip were treated for 24 hours with nanoparticles at IC<sub>50</sub> concentrations; 285.5  $\mu$ g/mL (*A. muricata*), 44  $\mu$ g/mL (*C. sappan*), or combination of both nanoparticles at IC<sub>50</sub>. The cells were then fixed using chilled methanol for 10 mins, washed with Phosphate Buffered Saline (PBS) three times, and 3% H<sub>2</sub>O<sub>2</sub> was used for quenching endogenous peroxidase activity. Cells were then incubated in blocking serum (bovine serum albumin) for 15 mins followed by washing with PBS. Mouse polyclonal anti-Bad antibody (cat#610392, BD Biosciences; diluted 1:100) was added as the primary antibody (1 h; RT). For secondary antibody, biotinylated goat anti-rabbit IgG (cat# BA-1000-1.5, Vector Lab; diluted 1:500) was added (15 mins, RT) after PBS flushing. Cells were then added with streptavidin (10 mins, RT), washed with PBS, then incubated with DAB buffer until the colour turned brownish. Cell nuclei were counterstained with Mayer's Hematoxylin for 5 mins and rinsed with distilled water. PBS was used to replace Bad polyclonal antibodies in the control group. Microscopy (Nikon) was performed using an objective lens at 40 $\times$ magnification. The cells that appeared brownish on their cytoplasm indicated successful binding of BAD

antibody with its antigen. Meanwhile, negatively stained cells showed purplish clear cytoplasm. The number of cells expressing BAD was scored based on their coverage in each field of view using the below formula. The mean of the percentage of area stained with BAD was calculated from five fields of view per slide. A total of thirty fields of view for each treatment group was observed.

$$BAD \text{ expression} = \frac{\text{positively stained cells}}{\text{total cells}} \times 100\%$$

#### Statistical analysis

The results were analyzed using SPSS 23 software (IBM), Mean  $\pm$  SD were calculated. Significance of differences was evaluated using Student's t-test. The differences between treatment groups and control were considered significant at  $p < 0.05$ .

## Results and Discussion

### Thin-Layer Chromatography Profile of Extract and Fraction of *A. muricata* Leaf and *C. sappan* Heartwood

The yield of extract and fraction from *A. muricata* leaf and *C. sappan* heartwood can be found as Supp. Table S2. The *A. muricata* leaf extraction using the percolation method with chloroform solvent and evaporated, resulted in a 5.9% sample yield of a thick and dark green extract. The extract was fractionated using Vacuum Liquid Chromatography (VLC) method with chloroform as a solvent. This process yielded 5.51% of fractions. Meanwhile, *C. sappan* heartwood extracted using the maceration method with methanol solvent resulted in a 5.69% sample yield of a thick, sticky, and reddish-brown extract. The fractionated *C. sappan* heartwood extract was then evaporated and produced 0.08% of a crusty and reddish-brown fraction. This colour might be originated from brazilin, which produces a typical reddish-brown colour when oxidized into water-soluble brazilin.<sup>15</sup> The fractionated extracts from both plants were subjected to TLC analysis and the profile results were grouped based on similarities in their hRf value (Table 1). Fractionation separates individual phytochemical groups.<sup>32</sup> The TLC plate of *C. sappan* heartwood appeared blue under UV366 nm light, indicating brazilin compounds.<sup>33</sup> Indeed, a previous study<sup>34</sup> showed that the Rf value of 0.67 suggests a phenolic compound such as brazilin. Meanwhile, the TLC plate of *A. muricata* leaf appeared red under UV366 nm, suggesting a possible polyketide derivative compound of the acetogenin group. Another study<sup>35</sup> showed that acetogenins are abundant in *A. muricata* with an Rf value of 0.79 $\pm$ 0.05. Brazilin and acetogenin are active compounds known to elicit cytotoxic effects against cancerous cell line.<sup>9,10,36</sup>

### Synthesis of nanoparticles from fraction of *A. muricata* leaf and *C. sappan* Heartwood

Studies involving nanoparticles have gained wide interest among researchers because the drug development on a nanoscale provides increased solubilization and absorption.<sup>37</sup> Nanoparticle formulation using chitosan as a polymer is expected to improve drug delivery ability. The addition of sodium tripolyphosphate (NaTPP) as a surfactant or cross-linker enhances stability and reduces the size of nanoparticles.

To determine the optimum formula, it is necessary to conduct a preliminary test to obtain the best ratio between chitosan and NaTPP. In this study, mixtures of chitosan and NaTPP were prepared in different ratio (3:1, 5:1, 6:1, 10:1, 11:1, 12:1, 13:1, 15:1, 17:1, 19:1 and 21:1) and their corresponding transmittance value were measured using spectrophotometry (Supp. Table S3).

The highest transmittance value (94.027%) was obtained at a ratio of 15:1 (Chitosan 93.74% and NaTPP 14.29%) and the lowest value at a ratio of 3:1 (Chitosan 85.71% and NaTPP 6.26%). The highest and lowest values were analyzed using the Design-Expert software, and the recommended 13 candidates of the formula are shown in Supplementary Table S4-S5.

Previous studies showed the effective in vivo dosage of *A. muricata* extract and *C. sappan* heartwood extract was 100 mg/kg BW

<sup>38</sup> and 25 mg/kg BW <sup>39</sup>, respectively. In this study, the dose of fraction added to the nanoparticle system was half of the effective dose *in vivo*. The fraction concentration of *A. muricata* and *C. sappan* nanoparticles used was 12.5 mg since *A. muricata* can only be dissolved in water at this concentration. From the 13 candidates of nanoparticle formulas, *A. muricata* nanoparticles were made using the formula of Chitosan + NaTPP + 12.5 mg *A. muricata* fraction + DMSO, whereas *C. sappan* heartwood nanoparticles were prepared using the formula Chitosan + NaTPP + 12.5 mg *C. sappan* fraction + aquadest. Tables 2 show the transmittance, particle size, and zeta potential values measured from nanoparticles of *A. muricata* leaf.

The Design-Expert software recommended the optimum formula to create nanoparticles of *A. muricata* leaf fraction with a desirable value of 0.639 with F<sub>opt</sub> = Chitosan 85.710% + NaTPP 14.290%. The software predicted that transmittance, particle size, and zeta potential values fall in the order, i.e., 87.2162% (transmittance), 317.415 nm (size), and 72.684 mV (zeta potential value). The actual readings for the above parameters were better than predicted, whereby the average transmittance readings were higher, and the average particle sizes and zeta potential value were lower (Table 2).

The optimum formula to create nanoparticles of *C. sappan* heartwood fraction with the desired value of 0.910 was F<sub>opt</sub> = Chitosan 90.606% + NaTPP 9.394%. With this desired value, it is possible that the fraction of *C. sappan* heartwood nanoparticles is very stable and will affect the uniformity of particle size distribution. The software predicted that transmittance, particle size, and zeta potential values ranged in order, i.e., 96.23% (transmittance), 320.533 nm (size), 66.6595 mV (zeta potential value). Similar to the *A. muricata* nanoparticle, the actual readings for transmittance and zeta potential in *C. sappan* nanoparticle were better than predicted. However, particle size measurement showed an average of 453.3 nm (Table 3), which is bigger than the predicted size. The difference in the actual readings might be attributed to some aggregation during storage which affects the particle size.

Nanoparticles are colloidal structures consisting of tiny particle sizes between 10-1000 nm.<sup>39</sup> Particle size is the most important characteristic in nanoparticle systems because it can determine the in vivo distribution, drug release, toxicity, and targeting ability of the nanoparticle system. In this study, the particle size obtained from the optimum recommended formula ranged from 207.5-587.7 nm, thus, has met the range of nanoparticle size. The transmittance value was measured over 90%, which means the nanoparticles' suspension was clear/less turbid. The polydispersity index (PI) estimates the range of particle size distribution in a sample and determines the presence or absence of aggregation. The particle size distribution is expressed as monodisperse if the PI is between 0.01-0.7.<sup>41</sup> The results in this study showed an average PI of approximately 0.328-0.547, indicating that the level of uniformity of the nanoparticle size distribution was quite good. The characteristics of the surface charge of nanoparticles are also an important feature to show the stability of a colloidal system, which is indicated by the zeta potential value. In general, nanoparticles with a zeta potential (+/-) 30 mV displayed stable suspensions.<sup>42</sup> Here, the zeta potential measurements were 66.46 mV (*A. muricata*) and 55.2 mV (*C. sappan*), indicating the possibility that these nanoparticle systems might be less stable.

**Table 1:** The hRf value of extract-fraction from *A. muricata* leaf and *C. sappan* heartwood

Sample	hRf
<i>A. muricata</i> extract	75 ; 70 ; 60 ; 40 ; 30 ; 20
<i>C. sappan</i> heartwood extract	82.5 ; 67.5 ; 62.5 ; 55 ; 32.5 ; 20 ; 15
<i>A. muricata</i> fraction	27.5 ; 15
<i>C. sappan</i> heartwood fraction	47.5 ; 32.5 ; 20 ; 12.5

**Table 2:** Transmittance, particle size, and zeta potential value of *A. muricata* leaf nanoparticles the from selected optimum formula (Chitosan 85.710% + NaTPP 14.290%)

Replication	Transmittance (%)	Particle size (nm)	Polydispersity Index	Zeta Potential (mv)
1.	92.033	207.5	0.328	65.7
2.	91.518	248.3	0.357	66.8
3.	92.768	256.9	0.377	66.9
Mean ± SD	92.106 ± 0.6	237.56 ± 26.3	0.354 ± 0.02	66.46 ± 0.6

**Table 3:** Transmittance, particle size, and zeta potential value of *C. sappan* heartwood nanoparticles the from selected optimum formula (Chitosan 90.606% + NaTPP 9.394%)

Replication	Transmittance (%)	Particle size (nm)	Polydispersity Index	Zeta Potential (mv)
1.	94.779	315.2	0.438	70.4
2.	97.062	457.1	0.547	54.3
3.	99.722	587.7	0.474	41.0
Mean ± SD	97.187 ± 2.4	453.3 ± 136.2	0.486 ± 0.05	55.2 ± 14.7

**Immunostaining of Bcl-2 Associated Agonist of Cell Death (BAD) protein**

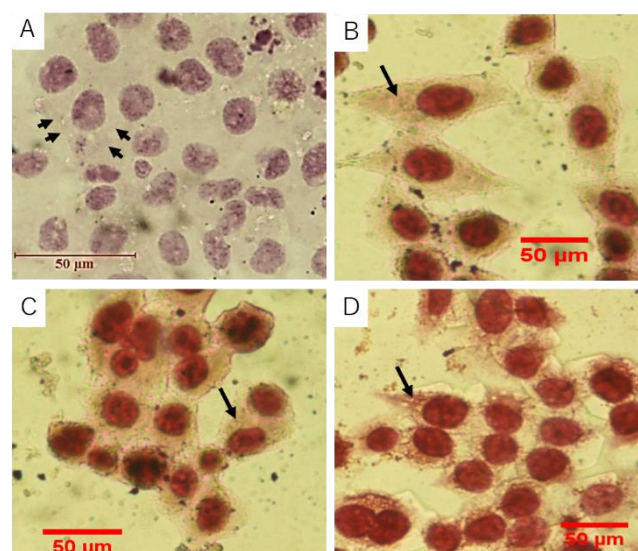
A preliminary study showed that nanoparticles from *A. muricata* leaf and *C. sappan* heartwood exhibited IC<sub>50</sub> values of 57.1 µg/mL and 88 µg/mL, respectively, suggesting a potential candidate of anti-cancer compounds. The expression of BAD pro-apoptotic protein in HeLa cells when exposed to doses of either nanoparticle of *A. muricata* leaf or *C. sappan* heartwood at IC<sub>50</sub> was then evaluated (Figure 1).

The immunocytochemistry staining of HeLa cells without nanoparticles treatment (control cells) demonstrated over 95% of cells were unlabeled with BAD, as shown by intact purplish colour in their nucleus and cytoplasmic surface (Table 4 and Figure 1A). Possibly, the absence of BAD expression in the control cells was because of the tumor suppressor gene inhibition by oncogenes E6 and E7 derived from HPV that impaired the apoptosis.<sup>43</sup> On the contrary, HeLa cells treated with *C. sappan* heartwood nanoparticles showed 80.49% apoptotic cells marked by BAD localization mainly in the cytoplasm (Table 4 and Figure 1B). The brownish cells indicate that endogenous BAD binds to the chromogen-tagged secondary antibody. BAD expression in HeLa cells may indicate the return of function of the tumor suppressor gene that signals cell death and upregulate the pro-apoptotic protein BAD. The number of apoptotic cells treated with *C. sappan* heartwood nanoparticles was much higher than the ones treated with *A. muricata* leaf nanoparticles (25.31%). This discrepancy might be attributed to the lower concentration of *A. muricata* used for nanoparticle synthesis as explained aforementioned, consequently resulting in less effective *A. muricata* nanoparticles. However, 50.3% of HeLa cells expressed BAD when both nanoparticles were combined (Table 4). This encourages us to further investigate if the combination of the two nanoparticles doses can act synergistically on regulating BAD-induced apoptosis.

The Bcl-2 associated agonist of cell death (BAD) protein involves in a complex regulatory pathway that initiates apoptosis. Cancer cells resist apoptosis by downregulating pro-apoptotic signals (e.g., BAD, BAX) and upregulating anti-apoptotic signals (e.g., Bcl-2, Akt, Mcl-1)<sup>17</sup>. Targeting antiapoptotic proteins by small-molecule inhibitors is a challenging task in cancer biology research due to the complexities in targeting many protein-protein interaction sites. A previous study<sup>44</sup> showed that molecular docking of phytochemicals found in *A. muricata* (acetogenin groups) exhibited strong binding interactions with Bcl-2 as compared to quercetin, the potent Bcl-2 natural inhibitors. The results suggest acetogenin could help promote the intrinsic pathway of apoptosis.<sup>44</sup> In line with this result, the present findings showed that *A. muricata* nanoparticle triggered BAD protein, perhaps by direct interaction of acetogenin and Bcl-2.

**Table 4:** The percentage of BAD-expressed HeLa cells in four different treatments

Treatment (IC <sub>50</sub> dose)	BAD expression (%)
Control	4.38 ± 0.04
<i>A. muricata</i> leaf nanoparticle	25.31 ± 0.6*
<i>C. sappan</i> heartwood nanoparticle	80.49 ± 0.3*
Combination	54.3 ± 0.7*

**Figure 1:** Immunostaining of HeLa cells with Bcl2-associated agonist of cell death (BAD).

(a) Control group, (b) cells treated with *A. muricata* leaves nanoparticles at IC<sub>50</sub> dose, (c) cells treated with *C. sappan* heartwood nanoparticles at IC<sub>50</sub> dose, (d) cells receiving combination dose of IC<sub>50</sub>. Note that cells in the treatment groups show strong cytoplasmic positivity (brownish colour shown by arrows). The nucleus of cells in the control was surrounded by purplish clear cytoplasm (arrowheads). \**p* < 0.05 in comparison to control. *N* = 30.

Activation of apoptosis via caspase-dependent pathway was reported in glioblastoma cells (U87) by anticancer properties of brazilin from *C. sappan*. Treatment with brazilin activates caspase-3 and subsequent cleavage of poly-(ADP-ribose) polymerase (PARP).<sup>36</sup> The future interest is to determine how HeLa cells are induced to undergo apoptosis and anticancer behaviors by corroborating BAD when treated with nanoparticles derived from either *A. muricata* or *C. sappan*.

#### Combined-dose of nanoparticles produces synergistic cytotoxic effect on HeLa Cells

Next, several doses of *A. muricata* leaf and *C. sappan* heartwood nanoparticles were combined to determine whether the combination exhibited synergism, antagonistic, or additive cytotoxic properties against HeLa cervical cancer. If the combination of the two shows synergism, it can reduce the use of the concentration of the two samples. The cytotoxic effect of the combined dose of nanoparticles is displayed in Figure 2.

The combination that resulted in the lowest HeLa cell viability (52.51%) was at 142.75 g/mL ( $1/4$  IC<sub>50</sub>) *A. muricata* leaf nanoparticle and 44 g/mL ( $1/2$  IC<sub>50</sub>) *C. sappan* heartwood nanoparticle (Figure 2). The morphology of HeLa cells 24-h after treatment with nanoparticles was observed using a light microscope (Supplementary Figure S1). Apoptotic HeLa cells showed cytoplasm shrinkage (arrow) and a decrease in cell volume. To the best of our knowledge, this result presents the first combination approach of *A. muricata* and *C. sappan* nanoparticles against cancer cells.<sup>4</sup> Previous reports had demonstrated synergistic therapeutic effects with the combination of acetogenin from *A. muricata*. For example, a combination of (2,4-*cis*)-10R-annonacin-A-one and (2,4-*trans*)-10R-annonacin-A-one showed cytotoxicity in breast cancer.<sup>44</sup> Combinations of acetogenin also exhibited cytotoxicity in the prostate (PC-3), renal (A498), and pancreatic (PACA-2) cancers.<sup>45</sup> To determine the relationship between nanoparticle doses and their cytotoxicity effect on HeLa cells, the combination index (CI) was calculated. Combining different doses of *A. muricata* nanoparticle and *C. sappan* nanoparticle revealed several CI values and criteria ranging from the synergistic effect to the antagonistic effect (see Supplementary Table S6-S7). Mild-moderate synergistic and synergistic effects are indicated by CI values in bold. Referring to the same mode of action, the most synergistic combination which produced the lowest CI value (0.39) was given by the combination of  $1/8$  IC<sub>50</sub> *A. muricata* leaf nanoparticles and  $1/10$  IC<sub>50</sub> *C. sappan* heartwood nanoparticles. Another synergistic combination was also obtained by combining a dose of  $1/4$  IC<sub>50</sub> *A. muricata* leaf nanoparticles and  $1/4$  IC<sub>50</sub> or  $1/10$  IC<sub>50</sub> *C. sappan* heartwood nanoparticles. In different modes of action, the most synergistic combination with a CI value of 0.42 resulted from the combination of  $1/8$  IC<sub>50</sub> *A. muricata* leaf nanoparticles and  $1/10$  IC<sub>50</sub> *C. sappan* heartwood nanoparticles. These data show that both nanoparticles, when combined in the right dose, can effectively kill HeLa cells compared to a single dose. In addition, it reduces the dose size for each nanoparticle. Each active compound has its role in regulating gene expression. However, some compounds have specific genes that work in the same direction, resulting in a synergistic effect. A higher synergistic effect correlates with a large number of specific genes that are affected in the same direction. Conversely, when more specific genes are affected in opposite directions, it will be directly correlated to a higher antagonistic effect.<sup>47</sup> Several factors may influence the performance of drug combinations, including the optimum time of drug exposure to determine gene expression and the selection of specific genes responsible for the direction of drug action, which is more inclined to synergistic or antagonistic effects. Other factors may also affect drug performance, e.g., the use of natural ingredients, where the activity is not only influenced by one entity but a mixture of various constituent components.<sup>48</sup>

Compared to single-drug therapy, multidrug therapy offers less risk to drug resistance and has less toxicity in small dosage combinations, as well as a higher therapeutic effect. It has gradually become the standard of care in cancer therapeutic areas. The present findings advanced our understanding of the nano-drug responsive cellular processes. Considering the potential application for a co-

chemotherapeutic agent, identification of the key mechanism that leads to the synergistic effect of *A. muricata* and *C. sappan* nanoparticles is highly desirable in the future.

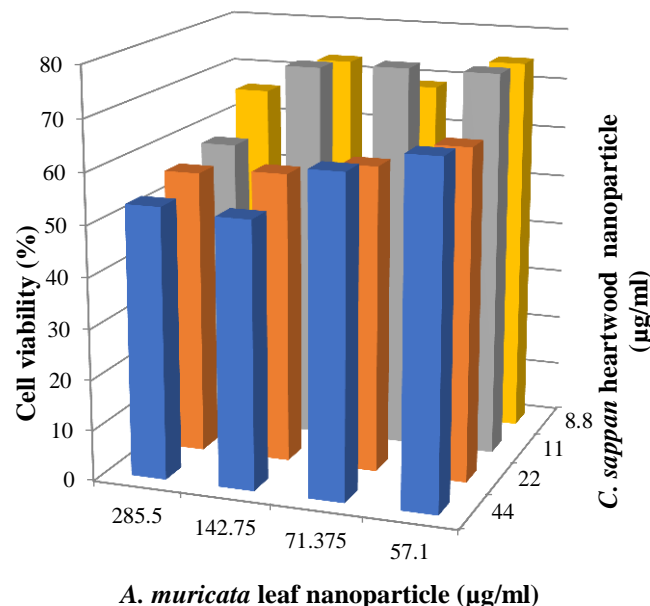


**Figure 2:** Cytotoxic effect of nanoparticles' combined dose on HeLa cells. Each nanoparticle was given at a series of concentrations, i.e.,  $1/2$  IC<sub>50</sub>,  $1/4$  IC<sub>50</sub>,  $1/8$  IC<sub>50</sub>, and  $1/10$  IC<sub>50</sub>.

#### Conclusion

In this study, a combination approach of applying nanoparticles from *A. muricata* and *C. sappan* against cancerous HeLa cells has been reported for the first time. The combined dose elicited a synergistic effect (CI<1) when each of the nanoparticle concentrations was given at a concentration  $1/2$  IC<sub>50</sub> and  $1/4$  IC<sub>50</sub>, thus, presenting an approach for efficient drug combination. The apoptotic pathway resulting in HeLa cell death after treatment with each nanoparticle was, at least, partly due to the upregulation of BAD protein.

#### Conflict of Interest

The authors declare no conflict of interest.

#### Authors' Declaration

The authors hereby declare that the work presented in this article is original and that any liability for claims relating to the content of this article will be borne by them.

#### Acknowledgments

We thank Suratman Suratman, M.Sc. from Sebelas Maret University for identifying the plant species.

#### References

- Choudhari A, Snehal S, Ruchika K-G. The aqueous extract of *Ficus Religiosa* induces cell cycle in human cervical cancer cell lines SiHa (HPV-16 Positive) and apoptosis in HeLa (HPV-18 Positive). PLoS One. 2013; 8(7):e70127.
- Singh S, Dhasmana DC, Bisht M, Singh PK. Pattern of adverse drug reactions to anticancer drugs: A quantitative and qualitative analysis. Indian J Med Paediatr Oncol. 2017; 38(2):140-145.
- Monsuez J-J, Charniot J-C, Vignat N, Artigou J-Y. Cardiac

- side-effects of cancer chemotherapy. *Int J Cardiol.* 2010; 144(1):3-15.
4. Astirin OP, Prayitno A, Artanti AN, Herawati E, Saad ANA, Firstlia AD. Single-dose and combined-dose of nanoparticles from soursop leaves (*Annona muricata* L.) and sappan wood (*Caesalpinia sappan* L.) induced apoptosis and necrosis in HeLa cells. *Pharmacogn J.* 2021; 13(5):1134-1142.
  5. Astirin OP, Prayitno A, Artanti AN, Fitria MS, Witianingsih DA, Pranatami DA, Putra ST. The expression of p53 and hsp70 proteins after treatment with *Annona muricata* Linn leaf for activating apoptotic and lead to homeostasis program of Raji cells. *Int J Cancer Ther Oncol.* 2014; 2(2):02028.
  6. Bukke AN, Hadi FN, Babu KS, Shankar PC. *In vitro* studies data on anticancer activity of *Caesalpinia sappan* L. heartwood and leaf extracts on MCF7 and A549 cell lines. *Data Brief.* 2018; 19:868-877.
  7. Artanti AN, Astirin OP, Prayitno A. Cytotoxic activity of non polar fraction from *Annona Muricata* L. leaves on HeLa and Raji Cell Line. *J Pharm Sci Clin Res.* 2016; 1(2):112-118.
  8. Najmuddin SUFS, RomLi MF, Hamid M, Alithen NB, Rahman NMANA. Anti-cancer effect of *Annona muricata* Linn leaves crude extract (AMCE) on breast cancer cell line. *BMC Compl Altern Med.* 2016; 16(1):1-20.
  9. Juang SH, Chiang CY, Liang FP, Chan HH, Yang JS, Wang SH, Lin YC, Kuo PC, Shen MR, Thang TD, Nguyet BT, Kuo SC, Wu TS. Mechanistic study of tetrahydrofuran-acetogenins in triggering endoplasmic reticulum stress response-apoptosis in human nasopharyngeal carcinoma. *Sci Rep.* 2016; 6:39251.
  10. Han B, Cao Yx, Li Zm, Wu Zx, Mao Yq, Chen Hl, Yao Zj, Wang Ls. Annonaceous acetogenin mimic AA005 suppresses human colon cancer cell growth in vivo through downregulation of Mcl-1. *Acta Pharmacol Sin.* 2019; 40:231-242.
  11. Kim BS, Chung TW, Choi HJ, Bae SJ, Cho HR, Lee SO, Choi JH, Joo JK, Ha KT. *Caesalpinia sappan* induces apoptotic cell death in ectopic endometrial 12Z cells through suppressing pyruvate dehydrogenase kinase 1 expression. *Exp Ther Med.* 2021; 21(4):357.
  12. Hung TM, Dang NH, Dat NT. Methanol extract from Vietnamese *Caesalpinia sappan* induces apoptosis in HeLa cells. *Bio Res.* 2014; 47(1):1-5.
  13. Yang X, Ren L, Zhang S, Zhao L, Wang J. Antitumor effects of purified protosappanin B extracted from *Lignum Sappan*. *Integr Cancer Ther.* 2016; 15(1):87-95.
  14. Wang SL, Cai B, Cui CB, Zhang HF, Yao XS, and Qu GX. Apoptosis induced by *Caesalpinia sappan* L. extract in leukemia cell line K562. *Chin J Cancer.* 2001; 20(12):1376-1379.
  15. NgamwonglumLert L, Devahastin S, Chiewchan N, Raghavan VGS. Colour and molecular structure alterations of brazilein extracted from *Caesalpinia sappan* L. under different pH and heating conditions. *Sci Rep.* 2020; 10:12386.
  16. Tao L, Li J, Zhang J. Brazilein overcame ABCB1-mediated multidrug resistance in human leukaemia K562/AO2 cells. *Afr J Pharm Pharmacol.* 2011; 5(16):1937-1944.
  17. Czabotar PE, Lessene G, Strasser A, Adams JM. Control of apoptosis by the BCL-2 protein family: implications for physiology and therapy. *Nat Rev Mol Cell Biol.* 2014; 15(1):49-63.
  18. Luna-Vargas MP and Chipuk JE. The deadly landscape of pro-apoptotic BCL-2 proteins in the outer mitochondrial membrane. *Federation Eur Biochem Soc J.* 2016; 283(14):2676-2689.
  19. Yu Y, Zhong Z, Guan Y. The downregulation of Bcl-xL/Bcl-2-associated death promoter indicates worse outcomes in patients with small cell lung carcinoma. *Int J Clin Exp Pathol* 2015; 8(10):13075-13082.
  20. Birkinshaw RW and Czabotar PE. The BCL-2 family of proteins and mitochondrial outer membrane permeabilisation. *Semin Cell Dev Biol.* 2017; 72:152-162.
  21. Pawlowski J and Kraft AS. Bax-induced apoptotic cell death. *Proc Nat Acad Sci of the USA.* 2000; 97(2):529-531.
  22. Xing X, He X, Peng J, Wang K, Tan W. Uptake of silica-coated nanoparticles by HeLa cells. *J Nanosci Nanotech.* 2005; 5(10):1688-1693.
  23. Kravanja G, Primožič M, Knez Ž, Leitgeb M. Chitosan-based (nano)materials for novel biomedical applications. *Molecules.* 2019; 24(10):1-23.
  24. Jiménez-Gómez CP and Cecilia JA. Chitosan: A natural biopolymer with a wide and varied range of applications. *Molecules.* 2020; 25(17):3981.
  25. Domenico L, Mikhail AK, Maria TC. Smart nanoparticles for drug delivery application: Development of versatile nanocarrier platforms in biotechnology and nanomedicine. *J Nanomaterials.* 2019(12); 1-26.
  26. Rubiyanto D. *Basic Techniques of Chromatography.* Yogyakarta: Deepublish; 2016; 130p.
  27. Oksal E, Pangestika I, Muhammad TST, Mohamad H, Amir H, Kassim MNI, Andriani Y. In vitro and in vivo studies of nanoparticles of chitosan-Pandanus tectorius fruit extract as new alternative treatment for hypercholesterolemia via Scavenger Receptor Class B type 1 pathway. *Saudi Pharm J.* 2020; 28(10):1263-1275.
  28. Buxton. *Design Expert.* [Online]. 2007 [cited 2020 Jul 31]. Available from: <https://www.lboro.ac.uk/media/media/schoolanddepartments/mLsc/downloads/Design-Expert-7.pdf>
  29. Cancer Chemoprevention Research Center. In vitro assay protocols. Cancer Chemoprevention Research Center UGM. [Online]. 2010 [cited 2019 Sept 26 ] Available from: [http://ccrc.farmasi.ugm.ac.id/?page\\_id=240](http://ccrc.farmasi.ugm.ac.id/?page_id=240).
  30. Reynolds CP and Maurer BJ. Evaluating response to antineoplastic drug combinations in tissue culture models. *Methods Mol Med.* 2005; 110:173-183.
  31. Michurina SV, Kolesnikov SI, Bochkareva AL, Ishchenko IY, Arkhipov SA. Expression of apoptosis regulator proteins Bcl-2 and Bad in rat ovarian follicular apparatus during recovery after extreme hypothermia. *Bull Exp Biol Med.* 2019; 168(2):205-209.
  32. Abubakar AR and Haque M. Preparation of medicinal plants: Basic extraction and fractionation procedures for experimental purposes. *J Pharm Bioallied Sci.* 2020; 12(1):1-10.
  33. Hung TM, Dang NH, Dat NT. Quality evaluation using TLC methods with reference to brazilein content of *Caesalpinia sappan* heartwoods in Thailand. *Songklanakarin J Sci Tech.* 2020; 42(1):196-202.
  34. Yemirta. Identifikasi kandungan senyawa antioksidan dalam kayu secang (*Caesalpinia Sappan*). *Jurnal Kimia dan Kemasan.* 2010; 32(2):41-46.
  35. Melot A, Fall D, Gleye C, Champy P. A polar Annonaceous acetogenins from the fruit pulp of *Annona muricata*. *Molecules.* 2009; 14(11):4387-4395.
  36. Lee DY, Lee MK, Kim GS, Noh HJ, Lee MH. Brazilein inhibits growth and induces apoptosis in human glioblastoma cells. *Molecules.* 2013; 18(2):2449-2457.
  37. Chaudhary S, Garg T, Murthy R, Rath G, Goyal AK. Development, optimization and evaluation of long chain nanolipid carrier for hepatic delivery of silymarin through lymphatic transport pathway. *Int J Pharm.* 2015; 485(1-2):108-121.
  38. Arthur FKN, Woode E, Terlabi EO, Larbie C. Evaluation of acute and subchronic toxicity of *Annona Muricata* (Linn.) aqueous extract in animals. *Eur J Exp Biol.* 2011; 1(4):115-124.
  39. Nugroho YA and Soeradi DO. Toksisitas akut dan efek pemberian ekstrak etanol kayu Secang (*Caesalpinia sappan*

- L) terhadap struktur anatomi tubulus seminiferus testis tikus putih. *Jurnal Bahan Alam Indonesia*. 2002; 1(1):35-39.
40. Prabha S, Arya G, Chandra R, Ahmed B, Nimesh S. Effect of size on biological properties of nanoparticles employed in gene delivery. *Artif Cells Nanomed Biotechnol*. 2016; 44(1):83-91.
41. Avadi MR, Sadeghi AMM, Mohammadpour N, Abedin S, Atyabi F, Dinarvand R, Rafiee-Tehrani M. Preparation and characterization of insulin nanoparticles using chitosan and Arabic gum with ionic gelation method. *Nanomed: Nanotech Biol Med*. 2010; 6(1):58-63.
42. Cosgrove T. *Colloid science principles, methods and applications*. (2nd ed). New York: Wiley. 2010; 363p.
43. Wulandari V. Association between oral contraceptives use and sexual activity with cervical cancer. *Jurnal Berkala Epidemiologi*. 2016; 4(3):432-442.
44. Antony P and Vijayan R. Acetogenins from *Annona muricata* as potential inhibitors of antiapoptotic proteins: A molecular modeling study. *Drug Des Dev Ther*. 2016; 10:1399-1410.
45. Wu FE, Zhao GX, Zeng L, Zhang Y, Schwedler JT, McLaughlin JL. Additional bioactive acetogenins, annomutacin and (2,4-Trans and Cis)-10R-Annonacin-A-Ones, from the leaves of *Annona muricata*. *J Nat Prod*. 1995; 58(9):1430-1437.
46. Torres MP, Rachagani S, Purohit V, Pandey P, Joshi S, Moore ED, Johansson SL, Singh PK, Ganti AK, Batra SK. Graviola: A novel promising natural-derived drug that inhibits tumorigenicity and metastasis of pancreatic cancer cells in vitro and in vivo through altering cell metabolism. *Cancer Lett*. 2012; 323(1):29-40.
47. Goswami CP, Cheng L, Alexander PS, Singal A, Li L. A new drug combinatory effect prediction algorithm on the cancer cell based on gene expression and dose-response curve. *CPT: Pharmacometrics Syst Pharmacol*. 2015; 4(2):80-90.
48. Wong KH, Lu A, Chen X, Yang Z. Natural Ingredient-Based Polymeric Nanoparticles for Cancer Treatment. *Molecules*. 2020; 25(16):3620.